CHANDRA
X-ray Center

MEMORANDUM

October 1, 1999

File: /data/acis0/svirani/ephin/reinhold/radbelt.tex

To: CXC, ACIS team, Project Science

From: S. N. Virani, R. Mueller-Mellin, P. P. Plucinsky

Subject: Using EPHIN's Detector Leakage Current To Understand Radiation Belt Transits

1 Introduction

The Electron Proton Helium Instrument (EPHIN) serves as a radiation monitor during the Chandra mission. It carries a total of 12 “scientific channels” which are sensitive to electrons, protons, and helium particles, in addition to an “integrated” channel. However, subsequent analysis has revealed that EPHIN's various channels saturate during a radiation belt transit. Therefore, these channels are of little utility if one is interested in understanding the radiation environment that Chandra is exposed to during perigee passage. Despite this shortcoming, there is one way to *crudely estimate* the behaviour during a given perigee crossing that allows us to compare one perigee crossing to another.

While the EPHIN electronics is driven into saturation due to several bottlenecks of different types [1], there is an analog housekeeping signal which is completely unaffected by saturation: the detector leakage current. One can use this leakage current as a proxy to understand the radiation belt environment from transit to transit.

There are six detector leakage currents on EPHIN, two of which are used in this analysis. Detector A leakage current (HKABIASLEAKI) has a nominal value between 150 and 200 nA. It is very temperature sensitive and will promptly react to changes as small as a few tenths of a degree. Even though the spacecraft thermal control keeps EPHIN in a narrow temperature range, the strong ionization by the high radiation environment inside the Van

Allen belts increases the leakage current to several hundred nA. Sometimes it even exceeds its conversion limit of 1 μA. The top panel of Figure 1 is a plot of the detector A leakage current versus time since IPS burn 3.

As detector A is heated by thermal solar input, its mean leakage current is higher than that of detector B. Therefore, examining the leakage current of detector B (HKB-BIASLEAKI), which has a lower nominal value of 30 nA thanks to its lower temperature, provides a better opportunity to understand the radiation belt environment. The bottom panel of Figure 1 is the corresponding detector B leakage current versus time plot. Notice that it does not reach its conversion limit during any perigee crossing.

Before proceeding to the results and analysis of this investigation, there are several caveats the reader should bear in mind. Firstly, to reiterate, only the B leakage current may be used for this analysis since the A leakage current frequently reaches its ADU conversion limit as Figure 1 illustrates. The A leakage current is also affected by temperature changes. Secondly, it is not possible to distinguish increases in the leakage current resulting from temperature increases to those produced by increases in the particle flux. However, *the B detector temperature should be quite stable even during perigee passages*. Thirdly, it is not possible to discern the spectrum of the particle flux from measuring the leakage current; only the total rate produced by ionizing particles can be measured. However, a minimum energy of 250 keV for electrons and 5 MeV for protons is necessary to penetrate detector A, the titanium foil, and the kapton foil. Lastly, it is not possible to separate the effects of variable spacecraft orientation and increased particle flux during belt transit.

2 Methodology

The procedure followed in this analysis is quite simple. Detector B leakage current versus time profiles for all radiation belt transits preceding the opening of the sunshade door (Day 224) were determined. The mean leakage current between radiation belt transits was also determined. This was found to be 0.0291 μA which was then subtracted from the entire data set so that the baseline is zero. The resulting profiles were then integrated to obtain

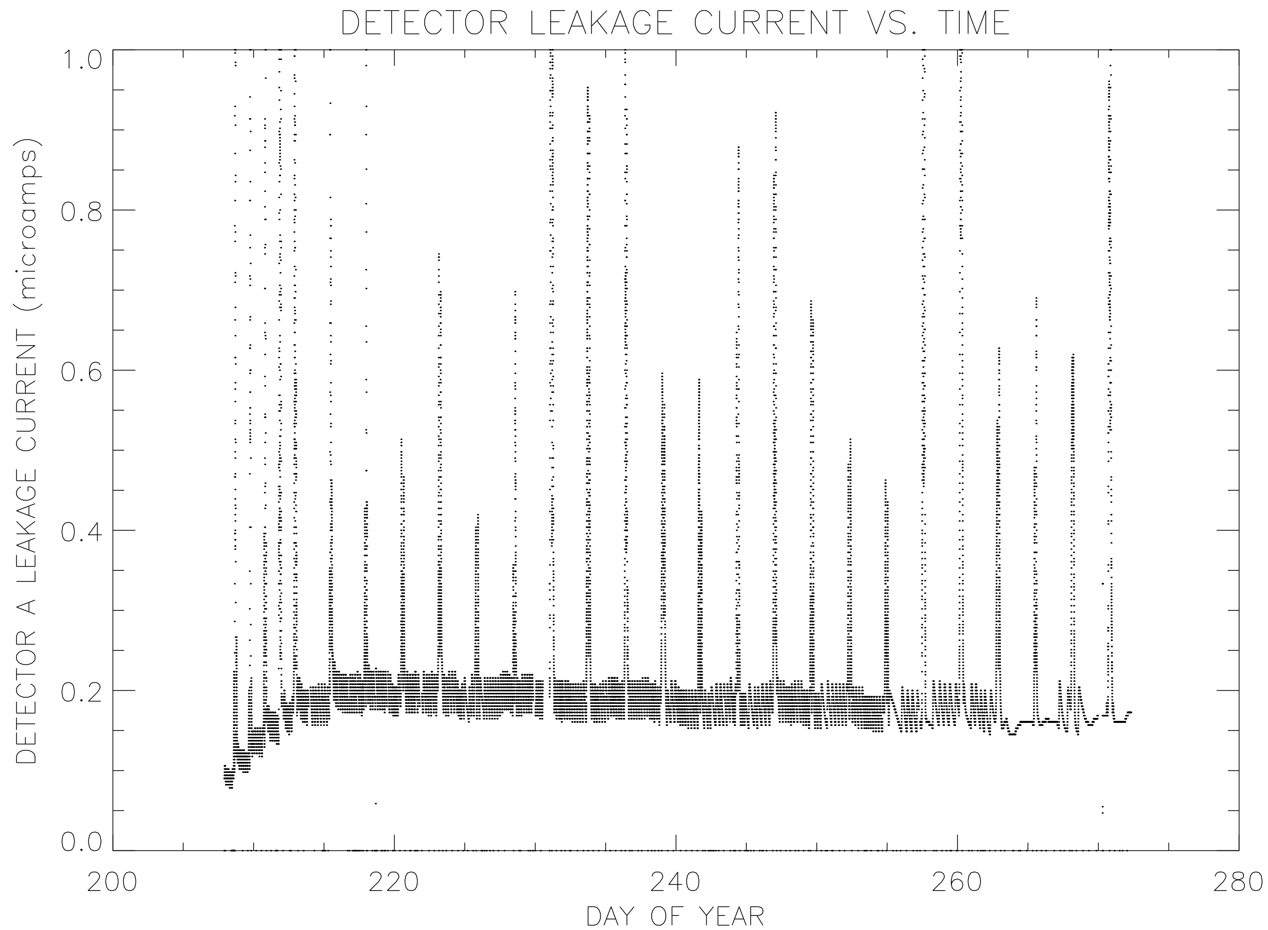

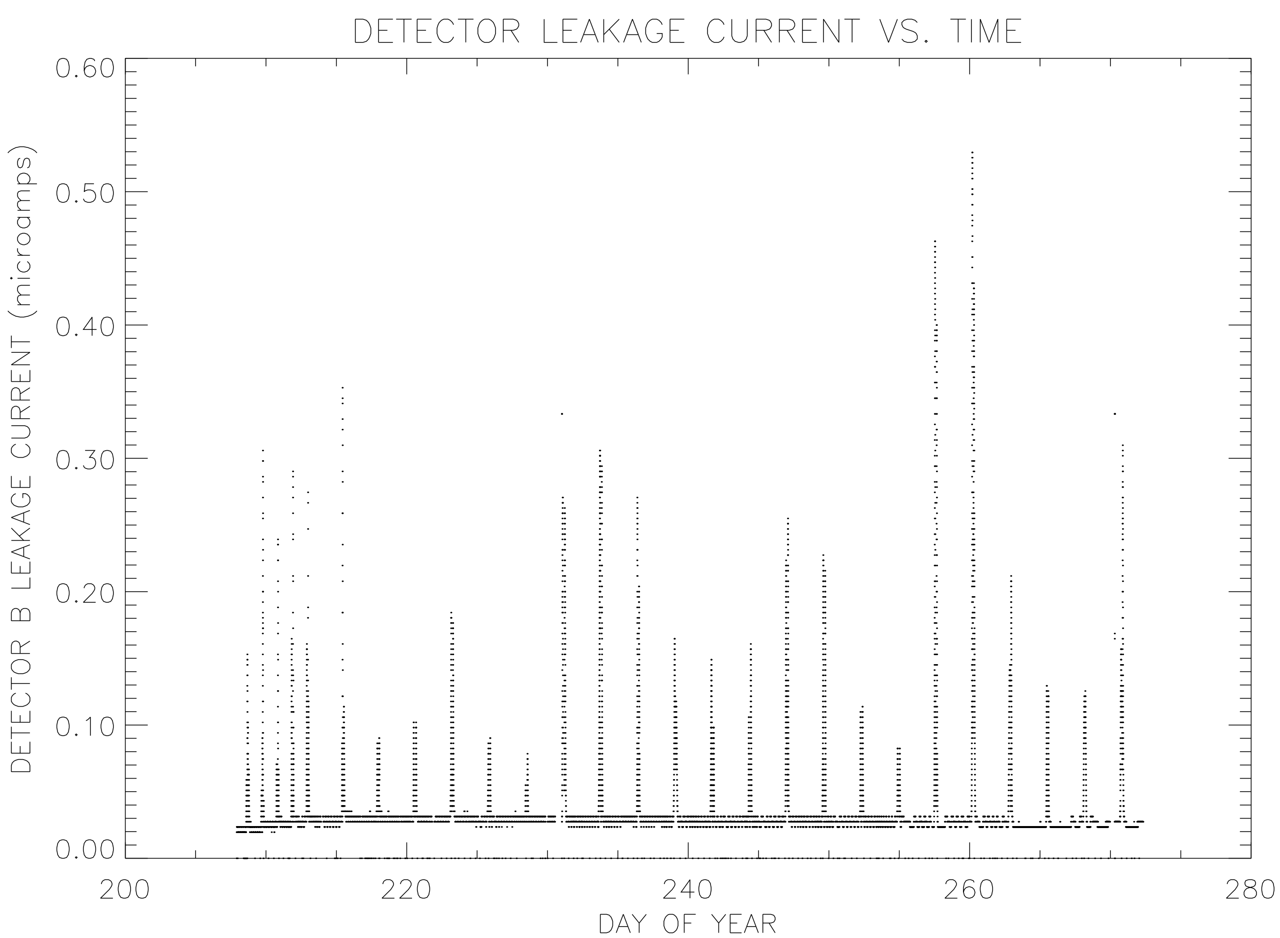

Figure 1: Leakage current since IPS 3.

the cumulative leakage current in a given perigee crossing which serves as an indicator for the radiation exposure.

3 Results and Analysis

This section will present B leakage current plots determined via the prescription given in the preceding section. Figure 2 presents four radiation belt transits – from Day 221 to Day 228. Note that the ACIS door was opened on Day 220 and the Sun-shade door was opened on Day 224.

Grade migration plots produced by several people (eg. A. Tennant, M. Markevitch, and T. Isobe) imply that the onset of ACIS CTI degradation began on or around Day 234/235. Figure 3 presents the A and B leakage current profile from Day 228 through till Day 240 inclusive. Figure 4 plots each of the radiation belt transits individually with their calculated integrated currents. Note that the spacecraft was in safe-mode and its instruments in the Sun-safe position during perigee crossing on Day 231.

From Day 240 to Day 255, there were 6 perigee crossings. Figure 5 is a 2 by 3 panel plot with each radiation belt transit isolated and its integrated current determined. Unfortunately, no analysis thus far has indicated how the CTI behaved during this time frame. It is believed that the analysis being performed by L. Townsley (ie, Au L line analysis) will provide the ACIS CTI behaviour during some of this time span. Until then, it is not possible to investigate the putative correlation between CTI degradation and perigee crossing in this time interval. However, B. McNamara has reported that between Days 224 and 259 inclusive, ACIS CTI degraded by two orders of magnitude [2].

In addition, C. Grant's CTI analysis of the Mn line energy demonstrates that from Day 259 till present, there has been no significant CTI degradation [3]. Similar to what was done above, Figure 6 is a plot of the B leakage current profile from Day 255 through till Day 272. Figure 7 is a 2 by 3 panel plot where each of the six radiation belt transits during that time span, for which there has been no reported CTI degradation, have been isolated and their integrated currents determined. Also, recall that during each perigee crossing since

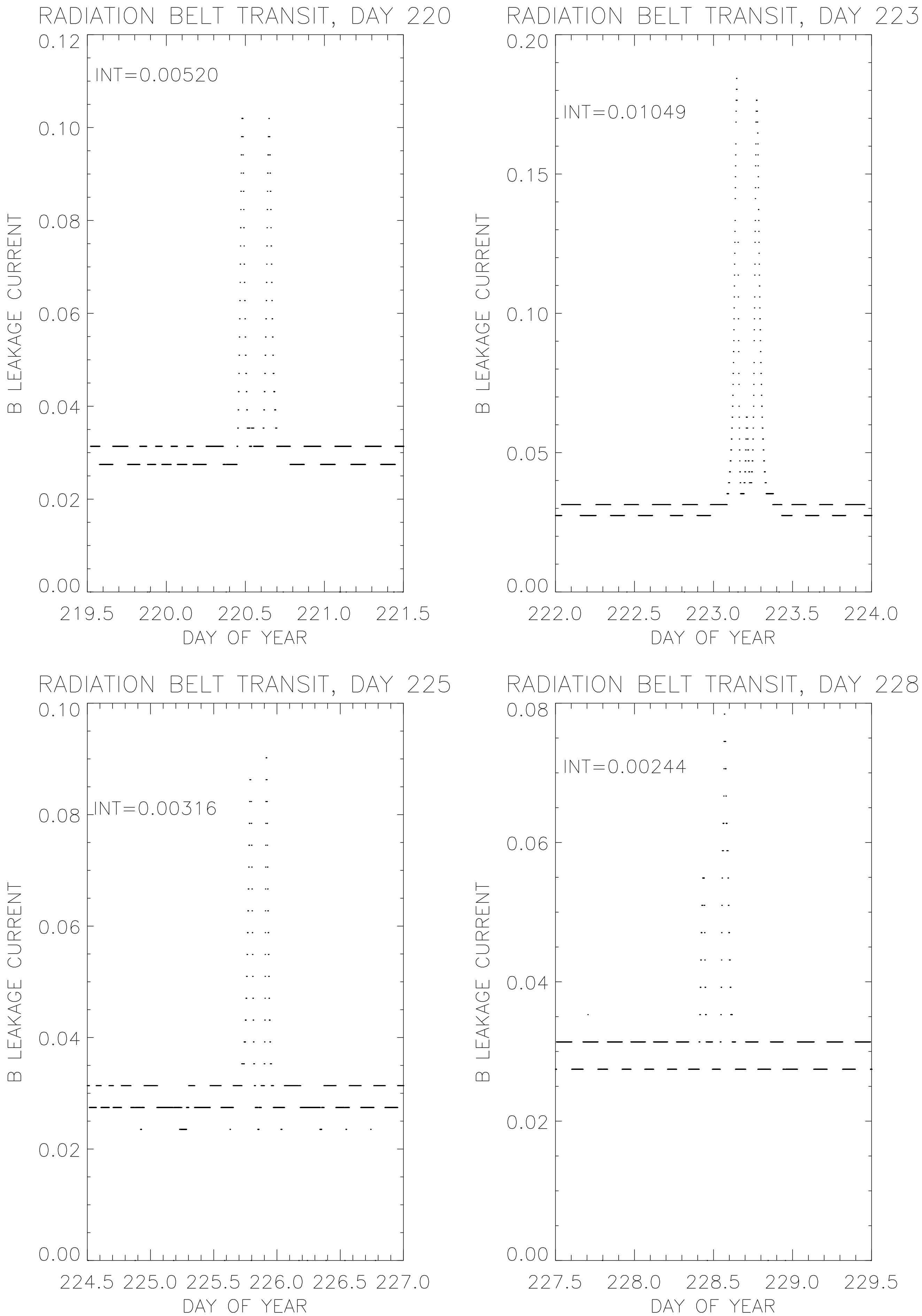

Figure 2: Leakage current during 4 radiation belt transits: Day 220 - Day 228.

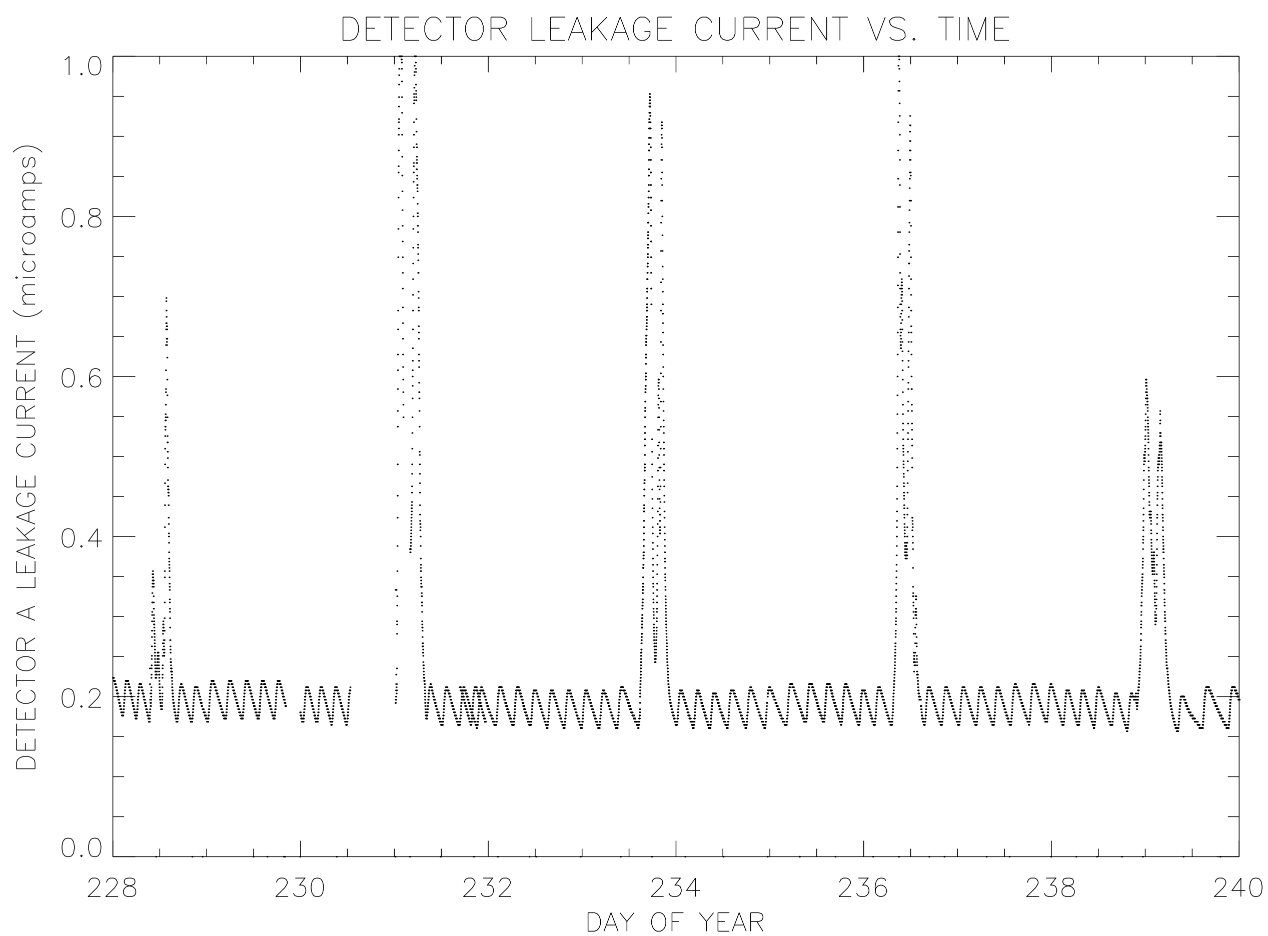

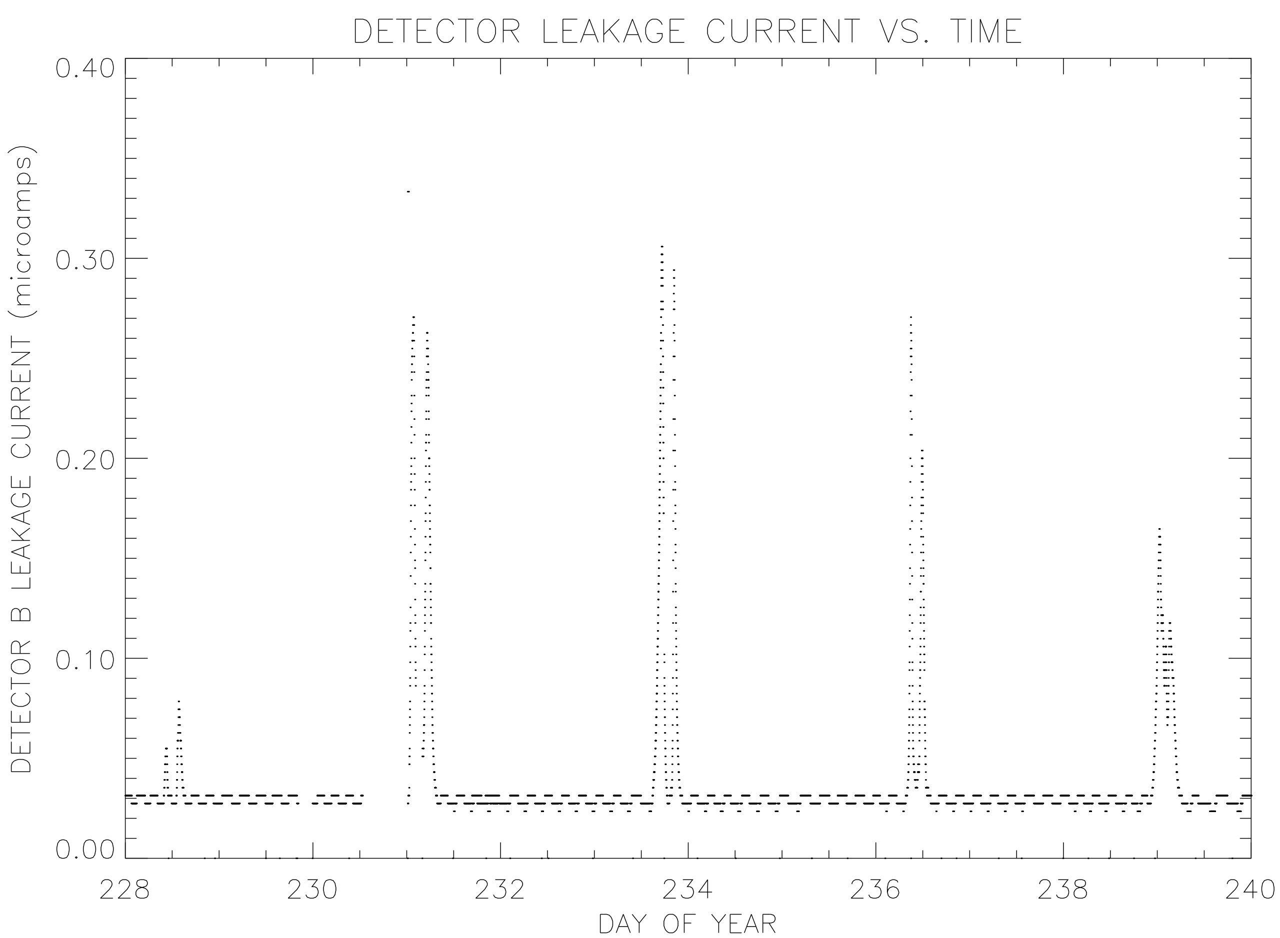

Figure 3: Leakage current soon after SSD opening: Day 228 - Day 240.

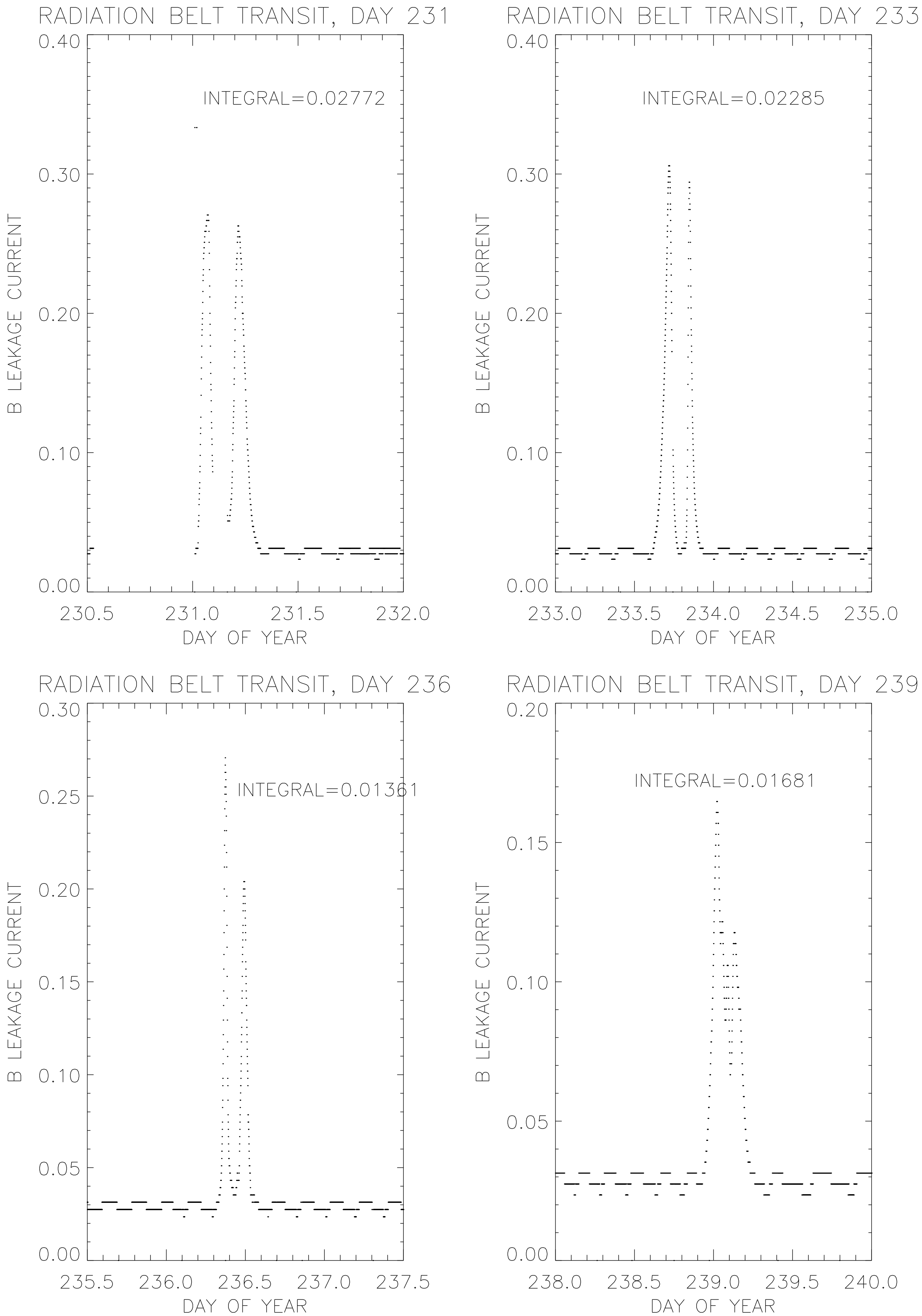

Figure 4: Leakage current during 4 radiation belt transits: Day 231 - Day 239.

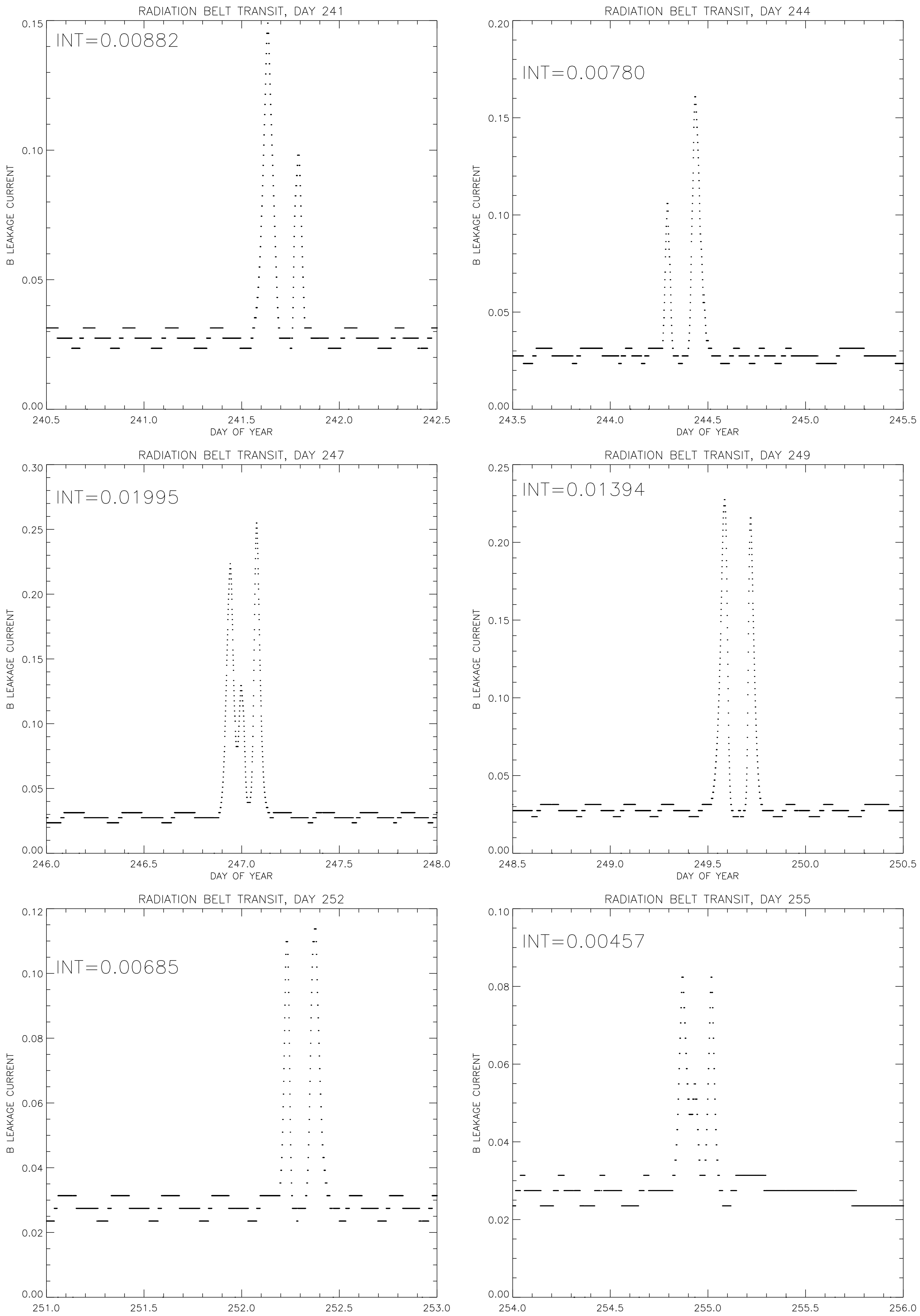

Figure 5: Leakage current during 6 radiation belt transits: Day 241 - Day 255.

Day 260, the spacecraft has been maneuvered into “eclipse configuration”. In addition, since perigee crossing 24 on Day 263, ACIS has been placed in the ’next-in-line position’ for each subsequent perigee crossing. Lastly, perigee crossings 16 (Day 241), 18 (Day 247), 23 (Day 260), and 26 (Day 268) also had the high energy transmission gratings (HETG) deployed.

Table 1 summarizes the information gleaned from the above plots. In addition to the integrated currents, also tabulated is the relative strength of a given perigee crossing with respect to a fiducial perigee crossing, as well as the focal plane instrument during that perigee crossing. For this analysis, the fiducial perigee crossing was taken to be the average integrated current of all radiation belt transits. The fiducial integrated current was found to be 0.01489. This now allows us to compare one transit to the next.

4 Conclusions

There are several points to be learned from this analysis. The first is that EPHIN can still be used to perform a relative comparison of the total particle flux experienced during radiation belt transits. However, information regarding particle species or their energies can not be determined. Second, in the total particle flux amongst perigee passages, there are significant differences. That is, there is approximately a factor of 20 difference between the strongest and weakest perigee crossing. Lastly, as M. Weisskopf points out in an email to the CTI-TASK distribution list [4], CTI analysis of S2 indicates that there was a significant change in CTI during a time interval that encompassed perigee crossings 21 and 22. Perigee crossing 22 has been the second strongest radiation belt transit according to this analysis. Furthermore, CTI analysis after perigee passage 22 indicates that there has been no measured change in CTI of S2. Table 1 demonstrates that during this same time frame, perigee crossings have been quite variable, with perigee crossing 23 being the strongest to date. However, recall that during this same time interval, it was decided to stow ACIS in the next-in-line position during perigee crossing. Also keep in mind that the HETG was deployed during perigee crossing 23. Lastly, in that same email from M. Weisskopf, he noted that there were statistically significant changes in the various metrics employed by C. Grant in her memo after perigee crossings. Regardless, it is clear that more data and analysis is still required to

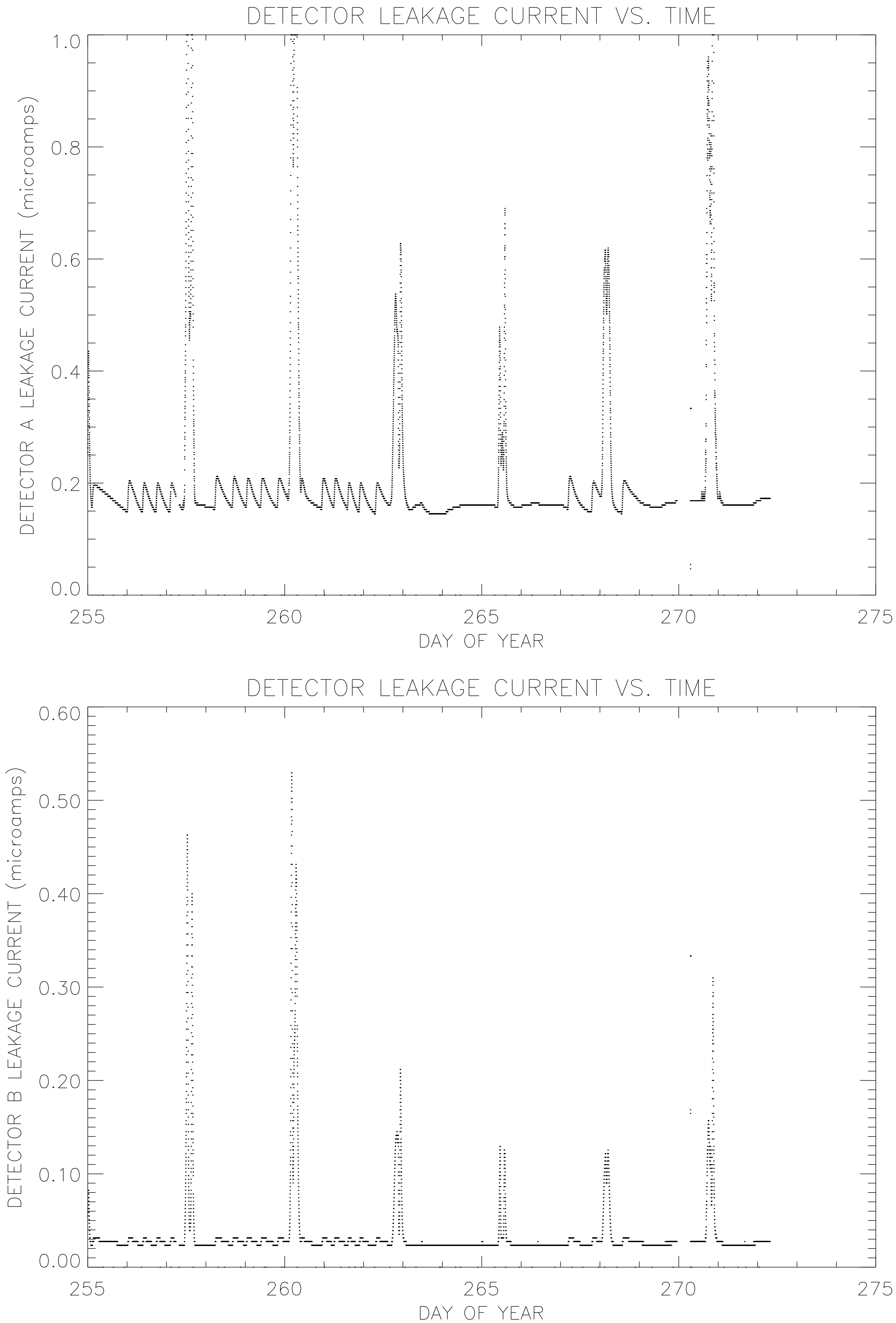

Figure 6: Leakage current when ACIS CTI has been stabilized: Day 255 - Day 272.

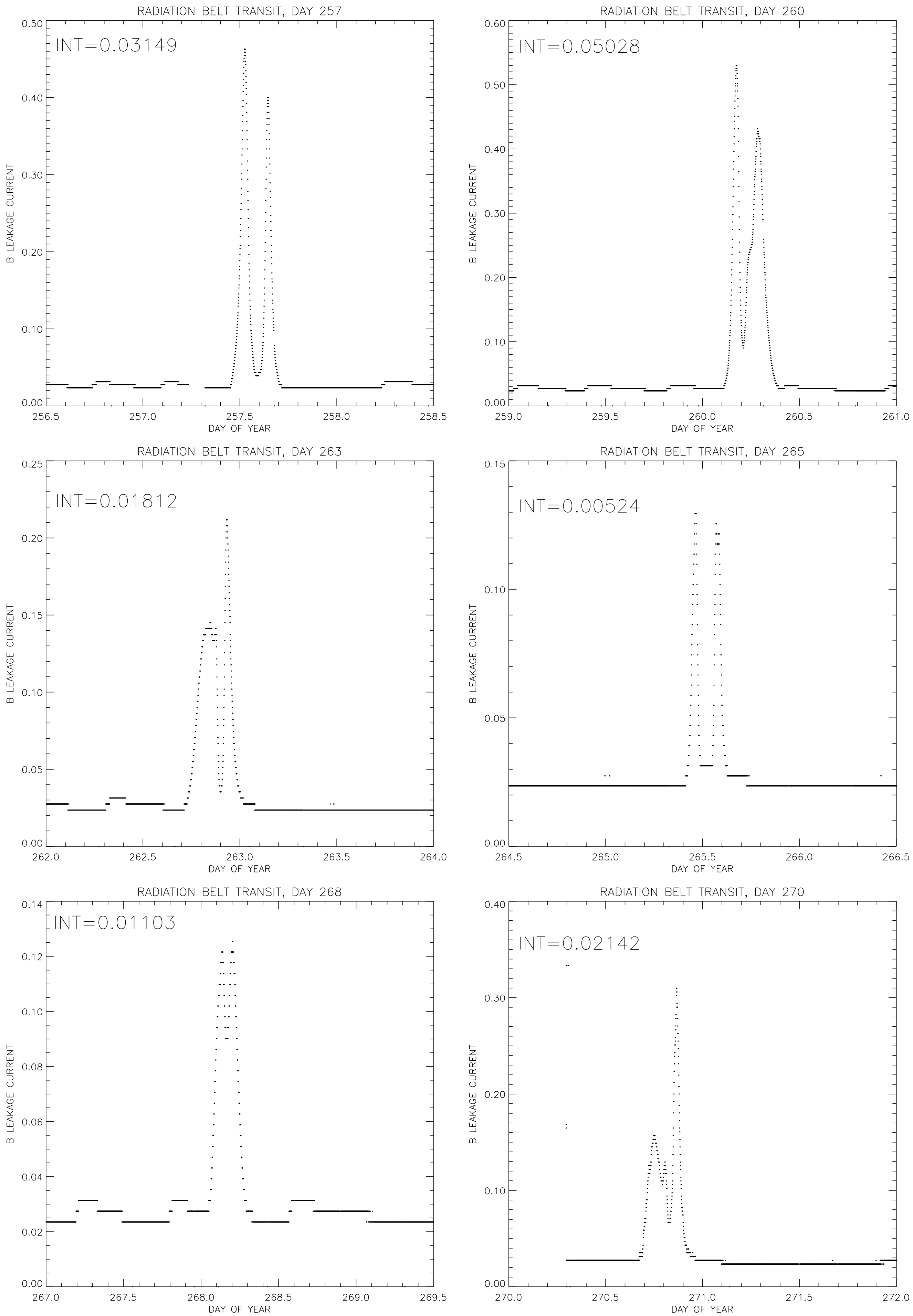

Figure 7: Leakage current during the last 6 radiation belt transits: Day 257 - Day 270.

Table 1: Integrated Current During Radiation Belt Transits and Their Relative Strengths

Day of Transit	Perigee Crossing	Integrated Current	Relative Strength	FP Instrument
220	8	0.00520	0.349	ACIS-S
223	9	0.01049	0.704	ACIS-S
225	10	0.00316	0.212	ACIS-S
228	11	0.00244	0.164	ACIS-S
231	12	0.02547	1.710	SAFE-MODE
233	13	0.02165	1.454	ACIS-S
236	14	0.01311	0.880	ACIS-I
239	15	0.01681	1.129	ACIS-I
241	16	0.00882	0.592	ACIS-S (HETG)
244	17	0.00780	0.524	HRC-I
247	18	0.01995	1.340	HRC-I (HETG)
249	19	0.01394	0.936	HRC-S
252	20	0.00685	0.460	ACIS-I
255	21	0.00457	0.307	ACIS-S
257	22	0.03149	2.115	ACIS-S
260	23	0.05028	3.376	$ACIS - S^1$ (HETG)
263	24	0.01812	1.217	$HRC - S^1$
265	25	0.00524	0.352	$HRC - S^1$
268	26	0.01103	0.741	$HRC - S^1$ (HETG)
270	27	0.02142	1.438	$HRC - S^1$

Column 1, Day of year of radiation belt transit ; Column 2, Perigee crossing number [4]; Column 3, Integrated current during transit (in units of μ-days; Column 4, Relative strength compared to a fiducial transit; Column 5, Focal plane instrument. Note [1] is to remind the reader that for these perigee crossings, Chandra was in "eclipse configuration".

firmly establish the correlation between perigee crossing and ACIS CTI degradation.

5 Future Work

Having established the leakage current as an effective proxy to probe the radiation belt environment that Chandra is exposed to with each perigee crossing, we intend to extend our investigation. What we will attempt to do is use detector leakage current A instead of B. Particles reaching detector B have to pass through the two foils and through detector A. Hence, detector B and its leakage current respond to higher energies (e $>$ 250 keV, protons $>$ 5 MeV). However, we are interested in as low an energy as possible. Since there is a very good correlation between detector A and B leakage currents, one can use the B leakage current to evaluate the A leakage current for those cases when A is above 1 μA. The utility in doing this is that dose measurements are easier to compare with CCD manufacturer specifications. Determining the A leakage current allows us to then correlate the A leakage current to the A00 counting rate. By then calculating the total exposure in terms of an orbit-averaged dose given in [particles/cm2] for electrons $>$ 200 keV and protons $>$ 2.5 MeV and then dividing by the A00 segment area, we can determine the radiation dose per perigee crossing for the ACIS CCD chips.

6 References

[1] Mueller-Mellin, R., 23 September 1999, private communication. [2] McNamara, B., 20 September 1999, email to CTI-TASK. [3] Grant, C., 23 September 1999, CTI Memo. [4] Weisskopf, M., 27 September 1999, email to CTI-TASK.